

## Development of a monoclonal antibody to a vibriophage as a proxy for *Vibrio cholerae* detection

Md. Abu Sayeed<sup>a\*</sup>, Taylor Paisie<sup>b</sup>, Meer Taifur Alam<sup>c</sup>, Afsar Ali<sup>a,c</sup>, Andrew Camilli<sup>d</sup>, Jens Wrammert<sup>e</sup>, Ashraful Islam Khan<sup>f</sup>, Firdausi Qadri<sup>f</sup>, Marco Salemi<sup>b</sup>, J. Glenn Morris<sup>c</sup>, Eric J. Nelson<sup>a,c,g</sup>

<sup>a</sup> Department of Environmental and Global Health, University of Florida, Gainesville, FL, USA

<sup>b</sup> Department of Pathology, University of Florida, Gainesville, FL, USA

<sup>c</sup> Emerging Pathogens Institute, University of Florida, Gainesville, FL, USA

<sup>d</sup> Department of Molecular Biology and Microbiology, Tufts University School of Medicine, Boston, Massachusetts, USA

<sup>e</sup> Department of Microbiology and Immunology, Emory University School of Medicine

<sup>f</sup> International Centre for Diarrhoeal Disease Research, Bangladesh (icddr,b), Dhaka, Bangladesh

<sup>g</sup> Department of Pediatrics, University of Florida, Gainesville, FL, USA

\* Corresponding author

Running title: Development of a monoclonal antibody to vibriophage

Keywords: Bacteriophage, vibriophage, phage, ICP1, *Vibrio cholerae*, cholera, Bangladesh, RDT, rapid diagnostic test, diarrhoea, diarrhea

Abstract: 224 words (250 max)

Text: 4257 words (5000 max)

Tables: None

Figures: 6

1 **ABSTRACT**

2 Cholera is an acute watery diarrheal disease that causes high rates of morbidity and  
3 mortality without treatment. Early detection of the etiologic agent of toxigenic *Vibrio*  
4 *cholerae* is important to mobilize treatment and mitigate outbreaks. Monoclonal antibody  
5 (mAb) based rapid diagnostic tests (RDTs) enable early detection in settings without  
6 laboratory capacity. However, the odds of an RDT testing positive are reduced by nearly  
7 90% when the common virulent bacteriophage ICP1 is present. We hypothesize that  
8 adding a mAb for the common, and specific, virulent bacteriophage ICP1 as a proxy for  
9 *V. cholerae* to an RDT will increase diagnostic sensitivity when virulent ICP1 phage are  
10 present. In this study, we used an *in-silico* approach to identify immunogenic ICP1  
11 protein targets that were conserved across disparate time periods and locations.  
12 Specificity of targets to cholera patients with known ICP1 was determined, and specific  
13 targets were used to produce mAbs in a murine model. Candidate mAbs to the head  
14 protein demonstrated specificity to ICP1 by ELISA and an ICP1 phage neutralization  
15 assay. The limit of detection of the final mAb candidate for ICP1 phage particles spiked  
16 into cholera stool matrix was  $8 \times 10^5$  plaque forming units by Western blot analysis. This  
17 mAb will be incorporated into a RDT prototype for evaluation in a future diagnostic study  
18 to test the guiding hypothesis behind this study.

## 19 INTRODUCTION

20 Cholera continues as one of the most important public health problems since 19th  
21 century, especially in resource-limited settings. Cholera can result in severe dehydration  
22 and death if untreated (1). The ongoing seventh cholera pandemic started in Indonesia  
23 in 1961 (2). Cholera remains endemic in regions of south-east Asia and Africa where  
24 there is a lack of safe drinking water, hygiene and improved sanitation (2, 3). It is  
25 estimated that 1.3 to 4.0 million cholera cases occur globally annually with 21,000 to  
26 143,000 deaths (1, 4, 5). The frequency of cholera outbreaks is likely to rise due to  
27 globalization, rapid urbanization, and climate change (6, 7). The causative agent for  
28 cholera is toxigenic *Vibrio cholerae*, a Gram-negative facultative anaerobe. *V. cholerae*  
29 can be classified into two biotypes, classical and El Tor, more than 200 serogroups (O1-  
30 O200), and two serotypes for O1, Ogawa and Inaba. Out of all serotypes, *V. cholerae* El  
31 Tor, O1, Ogawa and Inaba are the main etiologic agents for cholera outbreaks (8, 9).

32 Cholera outbreaks in endemic settings follow a seasonal pattern. During  
33 outbreaks, cholera patients shed hyper-infectious *V. cholerae* as well as virulent  
34 bacteriophages (phages) (10). The proportion of cholera positive stool samples carrying  
35 virulent phage likely increases over the course of an outbreak and can reach 100% (11).  
36 It is hypothesized that the predation of virulent phages influences the seasonal pattern  
37 of cholera epidemics in cholera endemic regions (10-13). Three primary virulent phages  
38 (ICP1, ICP2, ICP3) have been found in the stool of cholera patients in Bangladesh (14,  
39 15). ICP1, a member of *Myoviridae* bacteriophage family is the most prevalent phage  
40 excreted in cholera patient's stool during the episode of an epidemic (14, 16, 17). ICP1  
41 phage is specific to *V. cholerae* O1 and has been in other geographical locations

42 including India and Africa (South Sudan and Democratic Republic of Congo (DRC)) (16-  
43 19).

44 According to the World Health Organization, it is estimated that more than 90%  
45 of the annual cholera cases are not reported (20). The underestimation of cholera  
46 incidence acts as a barrier for planning and implementation of acute and long-term  
47 mitigation. Lack of resources for diagnostics and appropriate surveillance system in  
48 cholera prone areas is one of the major reasons for underreporting (2, 5, 21) and  
49 delayed public health response. A rapid and accurate point of care diagnostic test can  
50 expedite cholera surveillance, response and ultimately reduce mortality and morbidity  
51 (22-24).

52 The gold standards for cholera diagnosis are microbial culture and polymerase  
53 chain reaction (PCR) for the detection of *V. cholerae* from stool sample. However, the  
54 sensitivity of culture method alone is approximately 70% and requires at least 2-3 days  
55 in a well-equipped microbiology laboratory with trained personnel (16, 25-28). PCR for  
56 the detection of pathogens is an alternative to the culture because of its higher  
57 sensitivity of approximately 85% (8, 29). PCR is more rapid than conventional culture,  
58 but this technique requires expensive reagents and molecular equipment as well as  
59 trained laboratory staff.

60 Rapid diagnostic tests (RDTs) can be used by minimally trained staff at the bed  
61 side without requiring a cold-chain or advanced equipment. More than twenty cholera  
62 RDTs have been developed (20). Most are based on immunochromatographic  
63 immunoassays, targeting *V. cholerae* O1 lipopolysaccharide antigen (30-32). Laboratory  
64 and field evaluation of RDTs showed a wide range of sensitivity and specificity of

65 around 32 to 100% and 60 to 100%, respectively (4, 16, 24). RDT performance metrics  
66 are variable which largely limits their scope of use to cholera detection and surveillance.  
67 Our group has shown previously that virulent phage ICP1 and antibiotic exposure  
68 negatively impacts RDT performance. The odds of cholera RDT test positivity  
69 decreases by up to 90% when ICP1 phage are present (10, 16). To address this  
70 limitation, we hypothesized that adding an antibody for ICP1 to the RDT will be  
71 associated with an increase in sensitivity without compromising specificity when ICP1  
72 phage are present in cholera stool (Fig 1). In this study, we used *in-silico*, *in-vitro* and *in-*  
73 *vivo* techniques to develop a mAb that demonstrates specificity for the ICP1 phage, with  
74 the goal to incorporate the phage mAb into the RDT and evaluate the novel RDT in a  
75 future diagnostic study.

## 76 **METHODS**

77 **Clinical sample collection.** The sample collections analyzed were from previously  
78 published IRB approved studies; the recruitment, consent, enrollment and procedures  
79 are described (16, 19, 33, 34). In the first collection, stool samples from the Bangladesh  
80 study were obtained during September to December 2015 at a district hospital and a  
81 subdistrict hospital in the remote northern district of Netrokona (33). In the second  
82 library, stool samples from the South Sudan study were obtained during August to  
83 September 2015 at a cholera treatment center in Juba (34). The samples were collected  
84 prior to hospital administration of antibiotics; patient histories were negative for known  
85 antibiotic exposure. Lastly, microbiologic reagents were also obtained from a study in  
86 the Democratic Republic of Congo (19).

87 **Microbiologic procedures.**

88 *Bacterial strains, Phage, Media, and Growth Conditions.* We used the *V. cholerae* O1  
89 strain HC1037 to isolate and prepare virulent phages ICP1, ICP2 and ICP3. This strain  
90 naturally lacks K139 prophage and is sensitive to ICP1, ICP2 and ICP3. The bacterial  
91 strain was grown at 37°C in Luria-Bertani (LB) broth with aeration or on LB agar plates  
92 (10, 14). The bacterial strain and phages used in this study are listed in Table S1.

93 *Phage preparation, isolation, and plaque assays.* We used polyethylene glycol (PEG)  
94 precipitation method to make high titer phage stocks (15). *V. cholerae* was streaked on  
95 LB plate and incubated overnight at 37°C. A single colony from the plate was grown in  
96 LB broth to mid-exponential phase ( $OD_{600}=0.3$ ). Phages were added to the culture at a  
97 multiplicity of infection (MOI)=0.001 and incubated for 4-6 hours. The culture  
98 suspension was spun at 10,000 x g for 15 min at 4°C. After 0.2 µm filter sterilization of  
99 the supernatant, 0.25 volume PEG solution (20% PEG-8000; 2.5M NaCl) was added to  
100 the supernatant and incubated at 4°C for overnight for phage precipitation. Phages were  
101 pelleted by centrifugation at 10,000 x g for 25 min at 4°C. Phages were then washed  
102 with another round of PEG precipitation and finally resuspended in Phage80 buffer  
103 (0.085M NaCl, 0.1 mM MgSO<sub>4</sub>, 0.1 M Tris-HCl-pH 7.4). The titer of the phages was  
104 determined by plaque assay (10, 35). Phage preparation was serially diluted and  
105 incubated with mid-exponential *V. cholerae* culture for 10 min at room temperature. The  
106 mixture was added to soft LB agar (0.35% Agar) media and incubated at 37°C for 3-4  
107 hours until plaques were observed. The number of plaques were then calculated as  
108 plaque forming unit (PFU)/ml.

#### 109 **Molecular procedures.**

110 *Cloning, expression, and purification of recombinant target proteins.*

111 The putative baseplate protein (ORF75) and head protein (ORF122) of ICP1 phage  
112 were selected to clone and express in *Escherichia coli* (36-38). The open reading  
113 frames (ORFs) were amplified by PCR from genomic DNA. The primers were designed  
114 to include NdeI and XhoI restriction enzyme cutting sites at both ends of the amplified  
115 sequences. The PCR products and pET16b vector (Novagen) were digested with NdeI  
116 and XhoI at 37°C for 2 hours. The target sequences were cloned into pET16b by  
117 ligation using Quick Ligation™ Kit (NEB). After ligation, the recombinant plasmids were  
118 transformed into DH5 *E. coli* (Novagen) to make high copy plasmids. The cloned insert  
119 sequences were verified by colony PCR and DNA sequencing. The recombinant  
120 pET16b was then transformed into *E. coli* BL21 (Novagen) to express recombinant  
121 proteins as N-terminally His-tagged fusion proteins. A single transformed colony was  
122 picked to grow overnight at 37°C in LB broth containing 100 µg/ml ampicillin. The  
123 culture was diluted to OD<sub>600</sub> 0.1-0.2 and incubated at 37°C in LB broth for 2-3 hours  
124 until the OD<sub>600</sub> 0.5. Expression of recombinant proteins was induced for 4-6 hours at  
125 37°C by adding Isopropyl β-d-1-thiogalactopyranoside to the culture at a concentration  
126 of 0.1 mM. The culture was centrifuged at 5,000 x g for 15 minutes. Before purification,  
127 an aliquot of pellet suspension and supernatant were analyzed by sodium dodecyl  
128 sulfate–polyacrylamide gel electrophoresis (SDS-PAGE) to confirm the expression of  
129 desired proteins.

130 The recombinant proteins were purified using His•Bind® Purification Kit  
131 (Novagen) following manufacturer's instructions. In brief, the pellet was resuspended in  
132 Bugbuster reagent (5 ml/ gm of pellet) supplemented with Benzonase Nuclease (1  
133 µl/ml), lysozyme (1KU/ml) and protease inhibitor (10 µl/ml). The cell suspension was

134 incubated on a shaking platform at a slow setting for 20 minutes at room temperature  
135 (RT). After spinning at 16,000 x g for 20 minutes at 4°C, the supernatant was collected  
136 for analysis by SDS-PAGE. The pellet was resuspended and incubated again with same  
137 volume of Bugbuster reagent with lysozyme (1KU/ml) for 5 minutes at room-  
138 temperature (RT). After the addition of equal volume of 1:10 diluted Bugbuster reagent  
139 supplemented with protease inhibitor, the suspension was spun at 5,000 x g for 5  
140 minutes. The pellet was washed with 1:10 diluted Bugbuster reagent and centrifuged at  
141 16,000 x g for 15 minutes at 4°C. Proteins expressed as inclusion bodies were  
142 solubilized in 8 M urea. The lysate was mixed gently with 50% Ni-NTA His-bind slurry  
143 (EMD Millipore) at 4:1 ratio on a shaking platform for 60 minutes at RT. The lysate-resin  
144 mixture was carefully loaded into an empty column and washed 4 times with 8 M urea  
145 (pH-6.3). Monomeric recombinant proteins were eluted with 8 M urea (pH-5.9) and  
146 multimeric proteins were eluted with 8 M urea (pH-4.5). The purity of the proteins was  
147 further assessed by SDS-PAGE analysis and the protein concentration was measured  
148 using the Bradford method.

149 **Immunization and antibody production in cell culture.** The purified recombinant

150 ICP1 bacteriophage proteins were used to raise mAbs via a commercial vendor

151 (ProMab Biotechnologies, Inc.) using a conventional hybridoma technique (28).

152 Supernatants from 20 hybridoma clones for each of the two recombinant proteins from

153 were received from the vendor.

154 **Immunologic assays of monoclonal antibody candidates.**

155 *Enzyme linked immunosorbent assay (ELISA).* ELISA was used to screen the reactivity

156 of ORF75 and ORF122 specific-hybridoma clones to ICP1, ICP2 and ICP3 phages (39,



157 40). Nunc MaxiSorp plates were coated overnight at RT with ICP1 ( $10^3$  PFU/well), ICP2  
158 ( $10^3$  PFU/well), ICP3 ( $10^3$  PFU/well), formalin killed *V. cholerae* (VC;  $10^3$  CFU/well),  
159 ORF75 (200 ng/well), ORF122 (200 ng/well), and Bovine serum albumin (BSA; 200  
160 ng/well). BSA and VC were used as negative controls and recombinant ORF122 or  
161 ORF75 proteins were used as positive controls. After blocking with 1% BSA-PBS, the  
162 supernatants of ORF75 and ORF122 hybridoma clones were added to the wells at 1:20  
163 and 1:100 dilution, respectively and incubated for 1 hour at 37°C. Horseradish  
164 peroxidase-tagged goat anti-mouse IgG (Jackson ImmunoResearch) was added at  
165 1:1000 dilution to detect antigen bound IgG mAbs. We used chromogenic substrate, 1-  
166 Step<sup>TM</sup> Ultra TMB to develop color. After stopping the reaction with 2 N H<sub>2</sub>SO<sub>4</sub>, the  
167 absorbance was measured at 450 nm using ELISA plate reader. The absorbance  
168 corresponds to the antibody binding to the coated antigens.

169 *Western blot analysis.* The antigens were boiled with NuPAGE SDS sample buffer  
170 containing beta-mercaptoethanol for 10 min. The wells of NuPAGE 4-12% Bis-Tris  
171 precast gel (ThermoFisher) were loaded with ICP1 ( $10^8$  PFU/ well), ICP2 ( $10^8$  PFU/  
172 well), ICP3 ( $10^8$  PFU/ well), VC ( $5 \times 10^5$  CFU/well), ORF122 (2  $\mu$ g/well), ORF75 (2  
173  $\mu$ g/well) and BSA (2  $\mu$ g/well). To determine the limit of detection (LOD), we spiked ICP1  
174 in VC positive and ICP1 negative stool sample and prepared a 3-fold dilution series  
175 starting from  $10^8$  PFU/ well. After electrophoresis at 150 V for around 40-50 mins, the  
176 proteins from unstained gel were transferred to a nitrocellulose blotting membrane using  
177 Trans-Blot turbo Transfer System (Bio-Rad). The membrane was blocked with 5% skim  
178 milk in Tris buffered saline (TBS) for overnight at 4°C. To prepare primary antibody, the  
179 supernatants of hybridoma clones were diluted in 5% skim milk-TBS-Tw (0.1%) at 1:500

180 dilution. The primary antibody was added on the membrane and incubated for 1 hour  
181 with gentle shaking at RT. Following washing three times with TBS-Tw (0.1%), the  
182 membrane was incubated for 1 hour with the secondary antibody, alkaline phosphatase  
183 conjugated goat anti mouse IgG (1:5000 fold diluted in 5% skim milk-TBS-Tw) with  
184 gentle shaking at RT. The membrane was then washed three times with TBS-Tw (0.1%)  
185 and developed with 5-bromo-4-chloro-3-indolyl-phosphate/nitro blue tetrazolium  
186 (BCIP/NBT) substrate for around 5 minutes. The image of protein bands was captured  
187 in a gel imager (Geldoc; Bio-Rad).

188 *Phage neutralization assays.* Phage neutralization assays were developed and used to  
189 test neutralization/binding by each mAb to ICP1 in a biological context (41, 42). The  
190 mAbs were diluted to 20-fold in PBS and incubated with 60-100 PFU of ICP1, ICP2 and  
191 ICP3 for 1 hour at 37°C. The phage-sample mixture was added to an exponential *V.*  
192 *cholerae* culture (OD<sub>600</sub> 0.3) and incubated for 7-10 minutes at RT. The mixture was  
193 then added to soft LB agar (0.35% Agar) media and incubated at 37°C for 3-4 hours  
194 until plaques were observed. Phage neutralization was determined by comparing the  
195 plaque counts obtained from the assay without the mAb (only PBS).

196 **Statistical and bio-informatic analysis.** We used VaxiJen server (VaxiJen - Drug  
197 Design and Bioinformatics Lab) and IEDB tool (National Institute of Allergy and  
198 Infectious Diseases) for predicting possible antigenic ORFs of ICP1 bacteriophage (43,  
199 44). Clustal Omega (EMBL-EBI) was used for comparing the ORF75 and ORF122  
200 sequences of ICP1 genomes collected from different geographical locations. In order to  
201 compare how conserved ORF75 and ORF122 were in ICP1, alignments of 29 isolates  
202 from Bangladesh and Africa (DRC) were used; analyses were at both amino acid and

203 nucleotide levels. The data sets were used to construct a maximum likelihood (ML)  
204 phylogeny using the program IQ-TREE (45). The ML phylogeny was then used to  
205 assess temporal signal, using the program Temp-Est (46), in order to establish how  
206 conserved the ORF75 and ORF122 are in ICP1. The MSA alignment was then plotted  
207 using the R package ggmsa (<http://yulab-smu.top/ggmsa/>) and the temporal signal was  
208 plotted in R using ggplot2 and custom R scripts (47).

209 GraphPad Prism version 8 (GraphPad Software, Inc.) was used for statistical analyses  
210 and graphical presentation. The differences in antigen specific antibody responses were  
211 statistically evaluated by paired t-test. We also used the paired t-test to compare the  
212 antibody mediated phage neutralization with control. The differences were considered  
213 as statistically significant if  $p$  value was less than 0.05.

## 214 **RESULTS**

215 **Selection and characterization of ICP1 protein targets for monoclonal antibody**  
216 **production.** Eleven conserved ICP1 bacteriophage target open reading frames (ORFs)  
217 were identified and evaluated *in-silico* for immunogenic epitopes using VaxiJen and  
218 IEDB tools. The target ORFs were predicted to be highly antigenic with antigenicity  
219 scores of 0.54 to 1.03 (threshold of predicted antigen 0.4) by Vaxigen (Table S2). The  
220 targets were cross verified by IEDB to confirm antigenic epitopes (Table S2).

221 For further study, we selected the two putative structural proteins: a putative  
222 baseplate protein (ORF75) and a putative major head protein (ORF122). Analysis was  
223 performed on these targets to assess conservation by time and location. Conservation  
224 was found at both the nucleic acid and amino acids levels (Fig 2 A,B; Fig S2 A,B).

225 However, ORF75 demonstrated higher rates of genetic diversity over time (Fig 2C, Fig  
226 S2C) compared to ORF122 (Fig 2D, Fig S2D). The target ORF75 from the type-strain  
227 ICP1 from Bangladesh (ICP1\_2011\_A) showed 92% (709/774) similarity at the  
228 nucleotide level and 97% (249/257) similarity at the amino acid level compared to an  
229 ICP1 isolate from Africa (DRC; ICP1\_DRC\_106) by a Clustal Omega sequence  
230 alignment. The target ORF122 from the type-strain ICP1 from Bangladesh  
231 (ICP1\_2011\_A) showed 99.8% (1018/1020) similarity at the nucleotide level and 99.7%  
232 (338/339) similarity at the amino acid level compared to an ICP1 isolate from Africa  
233 (DRC; ICP1\_DRC\_106); see Supplemental material Fig S1.

234 For Figure 2A,B displaying the amino acid multi-sequence alignments (MSA), we  
235 detected a small amount of non-synonymous (dN) mutations. We observed more dN  
236 mutations in ORF75 than in ORF122. The temporal signal in Figure 2C,D highlights the  
237 conservation of ORF75 and ORF122; the temporal signal can infer whether or not  
238 accumulating mutations are observed over time and a dataset with an accumulation of  
239 mutations overtime would be displayed with a positive slope in the temporal signal plots.  
240 A neutral slope and negative slope were observed for ORF75 (Fig. 2D) and ORF122  
241 (Fig. 2D), respectively. Similar findings were observed at the nucleotide level (Fig. S2).

242 The ORF75 and ORF122 targets were screened (present/absent) by PCR in 12  
243 phage and *V. cholerae* negative (10 from Bangladesh and 2 from Africa (South Sudan)),  
244 2 ICP1 phage negative and *V. cholerae* positive (one from Bangladesh and one from  
245 Africa (South Sudan)), and 2 both ICP1 phage and *V. cholerae* positive stool samples  
246 (one from Bangladesh and one from Africa (South Sudan)). The ORFs were not  
247 detected in ICP1 negative stools (cholera or non-cholera). The ICP1 positive stools from

248 both Bangladesh and Africa (South Sudan) were positive for ORF75 and ORF122  
249 (Table S3).

250 **Evaluation of monoclonal antibody (mAb) candidates by ELISA.** Culture

251 supernatants of ORF75 hybridoma clones showed minimal to no reactivity to ICP1  
252 bacteriophage in contrast to positive reactivity with purified ORF75 protein; cross-  
253 reactivity to ICP2, and ICP3 was not detected (Fig 3A). In contrast, nineteen out of  
254 twenty culture supernatants of ORF122 hybridoma clones were reactive to ICP1 and  
255 purified ORF122; cross-reactivity to ICP2 and ICP3 was not detected. The relative  
256 responses to ICP1 were significantly higher in comparison to ICP2, ICP3, formalin-killed  
257 *V. cholerae* whole-cell (VCWC) and BSA; but was comparable with purified ORF122  
258 protein (Fig 3B). Given the failure of the ORF75 candidate mAbs to detect native ICP1,  
259 these candidates were eliminated from further analysis. Three ORF122 hybridoma  
260 clones including clone 5 (ICP1ORF122\_mAbCL5), clone 6 (ICP1ORF122\_mAbCL6)  
261 and clone 14 (ICP1ORF122\_mAbCL14) were selected for further analysis based on  
262 high reactivity to ICP1.

263 **Evaluation of head protein monoclonal antibody (mAb) candidates by Western**

264 **blot analysis.** The three candidate ORF122 hybridoma clone supernatants were  
265 analyzed by Western blot. All three clones detected ICP1 as well as purified ORF122  
266 recombinant protein. Cross-reactivity was not observed among the negative controls  
267 (ICP2, ICP3, VCWC, BSA, PBS; Fig 4A). All three candidate mAb clone supernatants  
268 detected ICP1 isolates from the disparate locations for Bangladesh and Africa (Goma  
269 DRC, Fig 4B).

270 **Evaluation of head protein monoclonal antibody (mAb) candidates by phage**

271 **neutralization assay analysis.** We characterized the three ICP1 reactive ORF122  
272 clone supernatants using a phage neutralization assay. All three mAb supernatant  
273 clones showed statistically significant neutralization of ICP1 (Fig 5); ICP1ORF122\_mAb  
274 CL5, CL6 and CL14 were able to neutralize 31%, 42% and 39% ICP1 bacteriophage,  
275 respectively in comparison to control (only PBS). The reduction in plaque counts by  
276 phage neutralization for all the clones were statistically significant ( $P<0.001$ ; Fig 5A).

277 **Limit of monoclonal antibody detection of ICP1 bacteriophage in cholera stool**

278 **matrix by Western blot analysis.** We determined the limit of detection of ICP1 phage  
279 for the two final candidate clone supernatants (ICP1ORF122\_mAb CL5 and CL6). We  
280 spiked ICP1 bacteriophage into ICP1 negative and *V. cholerae* negative stool samples  
281 in 3-fold dilution series. We found that both CL5 and CL6 culture supernatants (1:500)  
282 were able to detect down to  $8 \times 10^5$  PFU of ICP1 bacteriophage by Western blot (Fig 6).

283 **DISCUSSION**

284 In this study, we aimed to develop a mAb against the common virulent vibriophage ICP1  
285 as a critical step towards addressing limitations with current cholera RDTs. Our guiding  
286 hypothesis is that adding a mAb for ICP1 to the existing RDT as a proxy for *V. cholerae*  
287 will increase sensitivity when ICP1 degrades the primary *V. cholerae* target. We used  
288 an *in-silico* approach to identify immunogenic protein targets that were conserved and  
289 specific to cholera patients. Candidate proteins were expressed for mAb production,  
290 and mAbs to the head protein (ORF122) demonstrated specificity to ICP1 by both  
291 ELISA and a phage neutralization assay. The mAb to the head protein (ORF122) was  
292 able to detect ICP1 at biologically meaningful concentrations by Western blot analysis

293 when ICP1 was spiked into cholera stool matrix. This mAb will be incorporated into an  
294 RDT prototype for evaluation in a clinical study to test our guiding hypothesis.

295 This approach is innovative in that we sought to develop a mAb to a pathogen-  
296 specific phage as a proxy for the bacterial pathogen. However, the durability of the  
297 approach is vulnerable if the antigenicity of the epitope varies across time and place.  
298 The strong selective pressures between bacterial 'prey' and bacteriophage 'predator'  
299 drive elaborate mechanisms of phage immunity and escape, and ultimately genetic  
300 diversity. That said, genes for the candidate ICP1 structural proteins were found to be  
301 conserved. In prior analyses, the baseplate protein (ORF75) was conserved at near  
302 100% similarity and the head protein (ORF122) was conserved at more than 99%  
303 similarity at both amino acid and nucleic acid levels (17). With additional data, we found  
304 the baseplate gene for ORF75 was more divergent compared to ORF 122 across time  
305 and location. Both proteins are unlikely to be present in non-cholera patients given that  
306 the ORFs were not detected by PCR in non-cholera patient diarrheal stool, and cross-  
307 reactivity between phages is unlikely given that no significance sequence homology  
308 beyond ICP1 was identified, including within *Myoviridae*.

309 The other vulnerability of our approach is that the mAb might have cross-  
310 reactivity or degrade in cholera stool matrix which harbors proteases (48, 49).  
311 Monoclonal antibodies were raised to recombinant ORF75 and ORF122 proteins,  
312 however the mAb to the baseplate protein (ORF75) failed to bind native ICP1 by ELISA,  
313 Western blot and phage neutralization assays. This failure might be due to the lesser  
314 abundance of the epitope in the native ICP1 phage particle, post-transcriptional  
315 modification or possibly epitope masking. This is consistent with a previous study

316 showing that the staphylococcal phage major capsid protein was highly immunogenic,  
317 whereas the baseplate protein was found to be non-immunogenic in mice (50). On the  
318 other hand, the supernatants of the clones raised with the capsid protein ORF122 were  
319 reactive to the native ICP1 phage particle by ELISA, Western blot and phage  
320 neutralization assays. With respect to RDT development, the candidate mAbs were able  
321 to detect ICP1 alone, without cross-reactivity to ICP2 or ICP3. During western blot  
322 analysis, the cholera stool matrix with a ICP1 spike-in did not detectably interfere with  
323 ICP1 detection by the candidate mAbs.

324         These findings should be viewed within the context of the study limitations. First,  
325 the mAb did not fully ablate ICP1 in the viral neutralization assay. The mAb to ORF122  
326 reduced plaque formation by 30-40% ICP1 which was less than expected given its  
327 specificity. While this modest result is consistent with a similar study on anti-T4 head  
328 antibodies neutralizing T4 phage activity in *E. coli* (51), further optimization of the assay  
329 may be needed. Alternatively, the modest neutralization may be the result of cross-  
330 linking at the capsular head of ICP1 phage particles, which may leave the apparatus for  
331 binding and injection into the bacterial host operative (51, 52). Second, the scope of  
332 investigation of the mAb cross-reactivity was limited and will be improved upon by  
333 prototyping the RDT and a prospective diagnostic study in cholera and non-cholera  
334 patients. Third, we tested ICP1 spiked in cholera stool matrix alone and we did not have  
335 access to *V. cholerae* positive stool samples with or without ICP1 phage at native  
336 concentrations. While the limit of detection of ICP1 was lower than that anticipated in  
337 cholera stool, data are limited on the native concentrations of ICP1 across the time  
338 course of disease. Lastly, the exact epitopes that the mAbs bind remain unmapped.



339           Despite limitations, our work has significant implications. The mAb to the head  
340 protein (ORF122) developed herein can be used for making an enhanced RDT to detect  
341 ICP1 as a proxy for *V. cholerae*. In a prospective diagnostic study, we will evaluate the  
342 performance of the enhanced RDT across the course of cholera outbreaks given that  
343 cholera patients are more likely to shed virulent phage at the latter outbreak periods (11,  
344 12, 16).

345 **Acknowledgements**

346 We thank the patients for participating in the studies from which the clinical samples  
347 were obtained. We are grateful to Randy Autrey and Krista Berquist for their  
348 administrative expertise, as well as the UF Emerging Pathogens Institute and the UF  
349 Department of Pediatrics for providing vital infrastructure.

350 **Data availability**

351 Data analyzed are presented within the manuscript and online supplementary material.

352 **Financial Support**

353 This work was supported by a grant from the Wellcome Trust to EJM [DP5OD019893]  
354 and internal support from the Emerging Pathogens Institute, and the Departments of  
355 Pediatrics and the Department of Environmental and Global Health at the University of  
356 Florida, and by a grant from the NIH (USA) to AC [AI055058].

357 **Disclaimer**

358 The funders had no role in the study design, data collection and analysis, decision to  
359 publish, or preparation of the manuscript.

360 **Potential conflicts of interest.**

361 All authors: No reported conflicts.

362 TABLES:

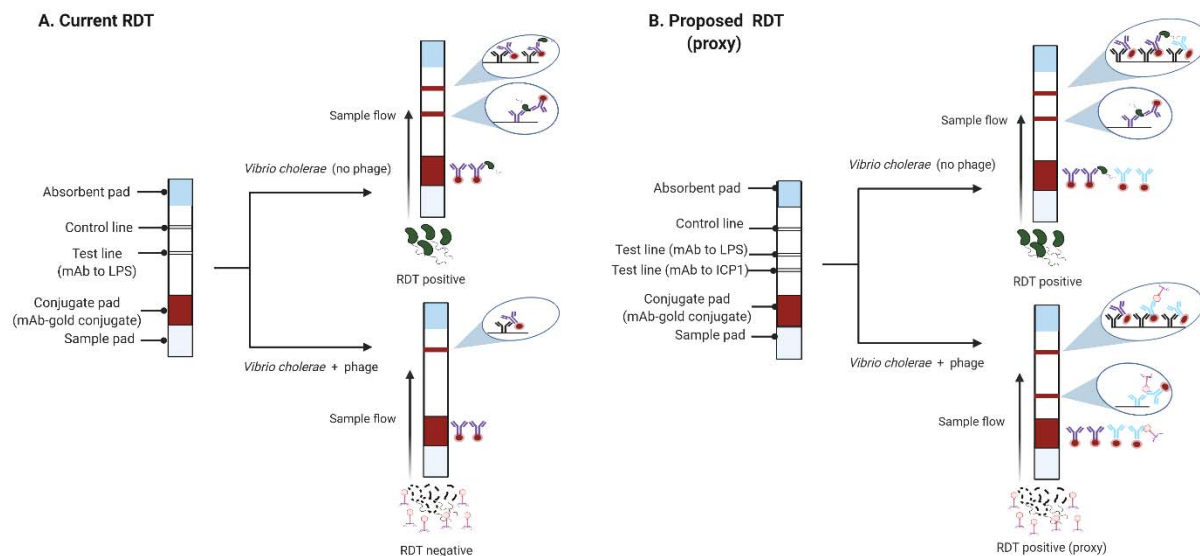
363 NONE

364

365 FIGURES 1-6

366

367 FIGURE 1



368

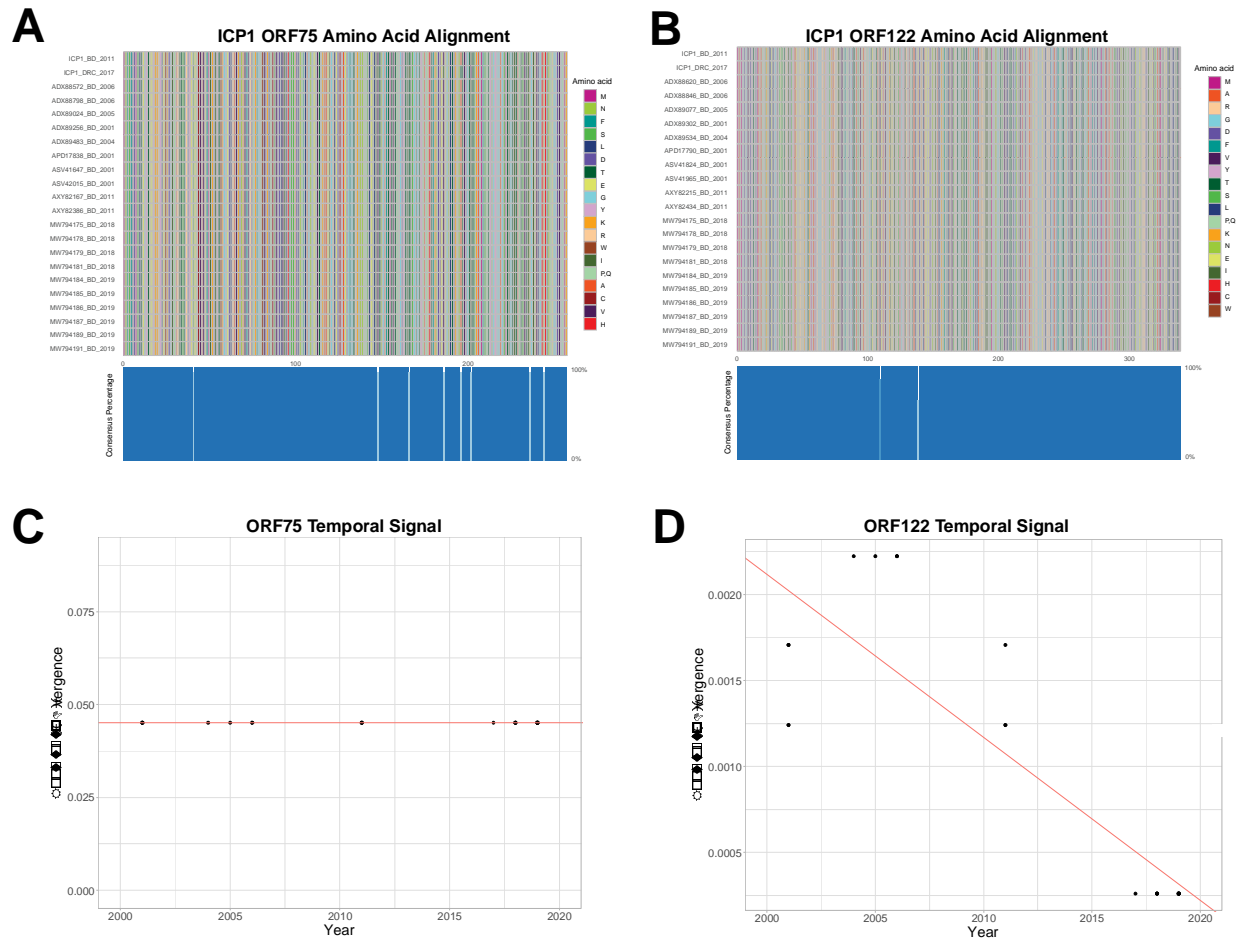
369 **Fig 1.** A model showing how an RDT for *V. cholerae* may fail when virulent phage (e.g.

370 ICP1) are present in a stool sample (A) and how this limitation can be addressed by

371 incorporating a mAb to phage as a proxy for *V. cholerae* when phage are present (B).

372

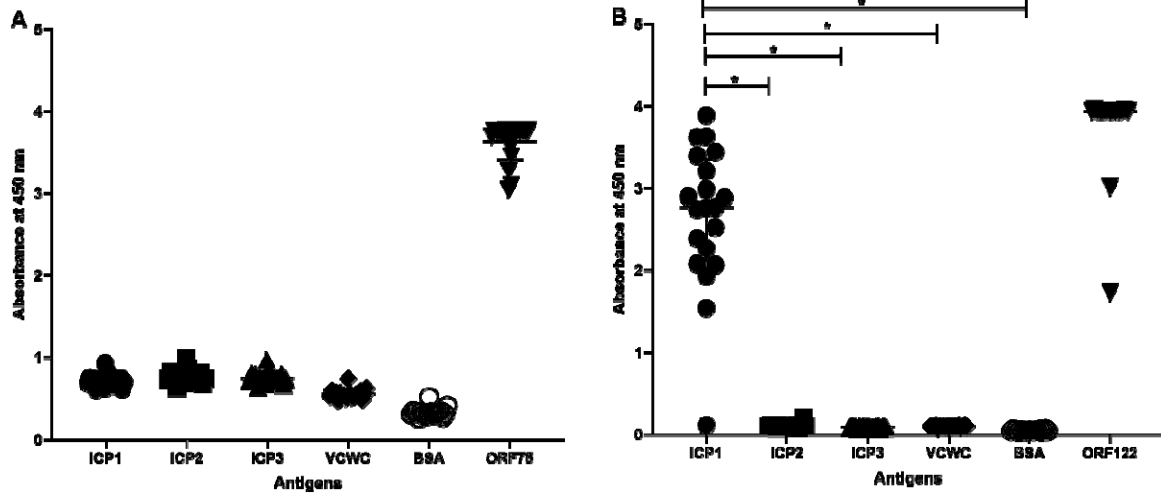
373 **FIGURE 2**



374

375 **Fig 2.** Multi-sequence alignment of ICP1 phage baseplate ORF75 **(A)** and capsular  
376 head ORF122 **(B)** amino acid sequences. Sequences from both Bangladesh (BD) and  
377 Democratic Republic of Congo (DRC). Blue boxes at the bottom of 'A' and 'B' represent  
378 the percentage of the isolates that have the same amino acid for that particular site.  
379 Temporal and divergence analysis of baseplate ORF75 **(C)** and capsular head ORF122  
380 **(D)** nucleotide sequences from ICP1 phage isolated from Bangladesh.

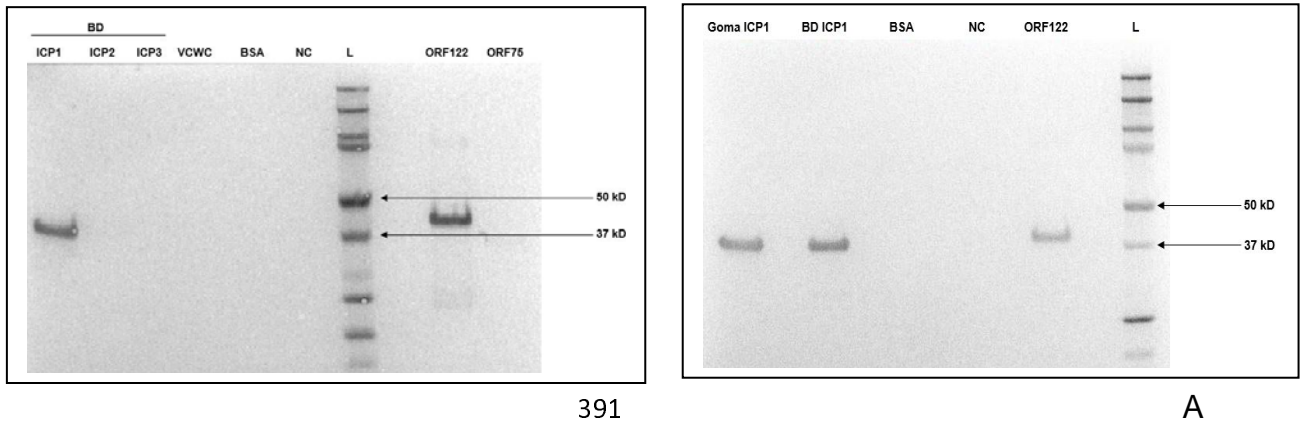
381 **FIGURE 3**



382

383 **Fig 3.** Immunoreactivity of ORF75 mAbs (n=20) (A) and ORF122 mAbs (n=20) (B) to  
384 phage particles (ICP1, ICP2, ICP3), formalin-killed *V. cholerae* whole-cell (VCWC),  
385 bovine serum albumin (BSA) and ORF75 and ORF122 recombinant protein. Statistically  
386 significant differences ( $P < 0.05$ ) in the mean immune response from all clones are  
387 denoted with an asterisk. Symbols represents the average of three technical replicates  
388 for one mAb from one experiment; data are representative of two independent  
389 experiments.

390 **FIGURE 4**

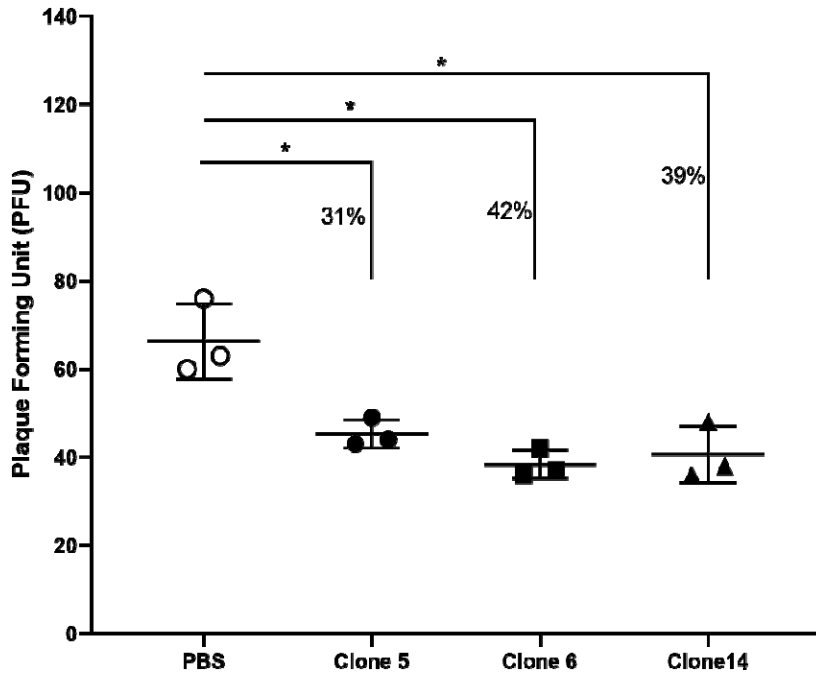


392 **B**

393 **Fig 4.** Western blot analysis of candidate ICP1ORF122\_mAbCL6 against ICP1 from  
394 Bangladesh (**A**) and Goma, DRC (**B**). Negative controls are ICP2 and ICP3. BD=  
395 Bangladesh, VCWC = formalin-killed *V. cholerae* whole-cell, bovine serum albumin =  
396 BSA, NC = negative control (only PBS), L = ladder (protein marker), ORF75 and  
397 ORF122 = ICP1 recombinant proteins.

399

400 **FIGURE 5**

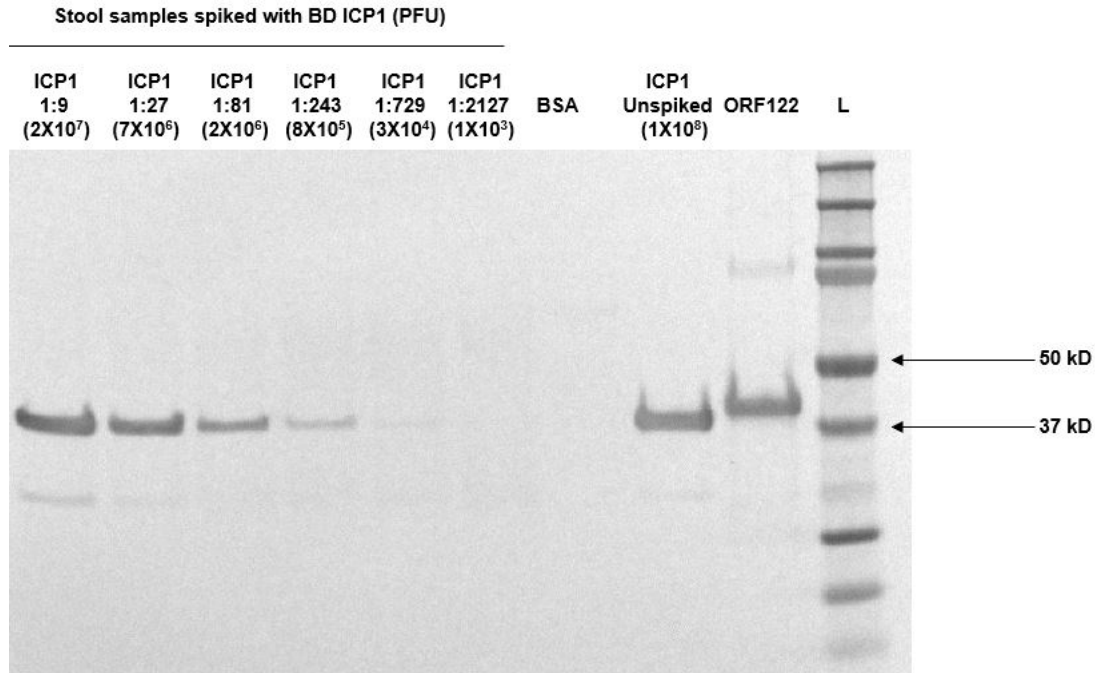


401

402 **Fig 5.** ICP1 phage neutralization by ICP1ORF122\_mAb CL5, CL6 and CL14. Here,  
403 PBS= phosphate buffered saline, ICP1ORF122\_mAb CL5, CL6 and CL14 represent  
404 culture supernatants from ORF122 hybridoma clones 5, 6 and 14, respectively. An  
405 asterisk denotes the statistically significant difference ( $P < 0.05$ ) in plaque counts when  
406 ORF122 mAb mediated neutralization responses are compared with the control (PBS).  
407 Each symbol represents the average of three technical replicates for one mAb from one  
408 experiment.

409

410 **FIGURE 6**



413 **Fig 6.** Determination of the limit of detection (LOD) of ICP1ORF122\_mAbCL6 against  
414 ICP1 in cholera stool supernatant. ICP1 was serially diluted in cholera stool known to be  
415 vibriophage negative (ICP1, ICP2, and ICP3 negative) in 3-fold dilution series. The  
416 concentration of the neat ICP1 stock was  $2 \times 10^{10}$  PFU/ml. The lane with 1:243 dilution  
417 represents  $8 \times 10^5$  PFU of ICP1 phage. Here, bovine serum albumin=BSA, ORF122=  
418 ICP1 recombinant protein and L= ladder (protein marker).

419

420



421 **SUPPLEMENTARY MATERIALS**

422 **FIGURE S1**

423

424

425

426

427

428

429

430

431

432

433

434

435

436

437

438

A.

ORF75_ICP1_Bd_Protein	MNFSFLDMSLTEGYTEEYKRYLEWKDGIPARITSTRDYEQCVAVEFMIKDIYTWKGG	60
ORF75_ICP1_Goma_Protein	MNFSFLDMSLTEGYTEEYKRYLEWKDGIPARITSTRDYETEQCVAVEFMIKDIYTWKGG	60
	*****	
ORF75_ICP1_Bd_Protein	EDLRAVKLNKVFVRLPKFGPWVKLPCSVDDLVLHFSSKDLNQFLAGNGEQVTQKAAEI	120
ORF75_ICP1_Goma_Protein	EDLRAVKLNKVFVRLPKFGPWVKLPCSVDDLVLHFSSKDLNQFLAGNGEQVTQKAAEI	120
	*****	
ORF75_ICP1_Bd_Protein	GELEDGYAELGFGTRKSNQPSLENLIVTNGAF TMTVTPQGDYTIITSGTGTYQAQKHTF	180
ORF75_ICP1_Goma_Protein	GELEDGYAELGFGTRKSNQPSLENLIIITNGAF TMTVTPQGDYTIITSGTGTYQAQKHTF	180
	*****	
ORF75_ICP1_Bd_Protein	KNDVEVEGNLTVKQNTVDGTITSKAGMFSPTYSYGGAGSMTIGTITAQTSVTINGIEV	240
ORF75_ICP1_Goma_Protein	KNDVEIEGNLTVKQNTVDGTITSKAGMFSPTYSYGGAGSMTIGTITAQTSVTIDGIEV	240
	*****	
ORF75_ICP1_Bd_Protein	LGHKHTNPEGGDVGPMPK	257
ORF75_ICP1_Goma_Protein	LGHKHTNPEGGDVGPMPK	257
	*****	

430

431

432

433

434

435

436

437

438

B.

ORF122_ICP1_Bd_Protein	MARMGDFGVVDYTSMLALAPRSKNFLELLGVFSESNTRYIDSRYAEEFEREEKGVTKMNAM	60
ORF122_ICP1_Goma_Protein	MARMGDFGVVDYTSMLALAPRSKNFLELLGVFSESNTRYIDSRYAEEFEREEKGVTKMNAM	60
	*****	
ORF122_ICP1_Bd_Protein	ARGGSRKYIGSEKARKEIIEVPFAPLDGVTVASEVEAFRQYGTESQTASIEALVQRKIEH	120
ORF122_ICP1_Goma_Protein	ARGGSRKYIGSEKARKEIIEVPFAPLDGVTVASEVEAFRQYGTESQTASVEALVQRKIEH	120
	*****	
ORF122_ICP1_Bd_Protein	IQRSHGIYIRDCQYTALLEDKILAEDEDGNEITALAKNFSTLWGVSRKTGAINTTTAVNP	180
ORF122_ICP1_Goma_Protein	IQRSHGIYIRDCQYTALLEDKILAEDEDGNEITALAKNFSTLWGVSRKTGAINTTTAVNP	180
	*****	
ORF122_ICP1_Bd_Protein	FSVLATKRQEIIDSMGENNGFTSMVVLCTTRDFNAIVDHPDVRAAYEGRDGGAEYLTRRL	240
ORF122_ICP1_Goma_Protein	FSVLATKRQEIIDSMGENNGFTSMVVLCTTRDFNAIVDHPDVRAAYEGRDGGAEYLTRRL	240
	*****	
ORF122_ICP1_Bd_Protein	GDAVDFQVFTHKGVTLVEDTSGKLTGDSAYMFLGVQDMFQAVYAPADSTDHVNTISQGS	300
ORF122_ICP1_Goma_Protein	GDAVDFQVFTHKGVTLVEDTSGKLTGDSAYMFLGVQDMFQAVYAPADSTDHVNTISQGS	300
	*****	
ORF122_ICP1_Bd_Protein	YLFLNAGENWRRDVEIESEVSYACMVTRSELICDLTITVA	339
ORF122_ICP1_Goma_Protein	YLFLNAGENWRRDVEIESEVSYACMVTRSELICDLTITVA	339
	*****	

439 **Fig S1.** Alignment of Bangladesh (Bd) (14) and Goma ICP1 (19) bacteriophage ORF75

440 (A) and ORF122 (B) protein sequences by Clustal Omega (EMBL-EBI). Alignment is

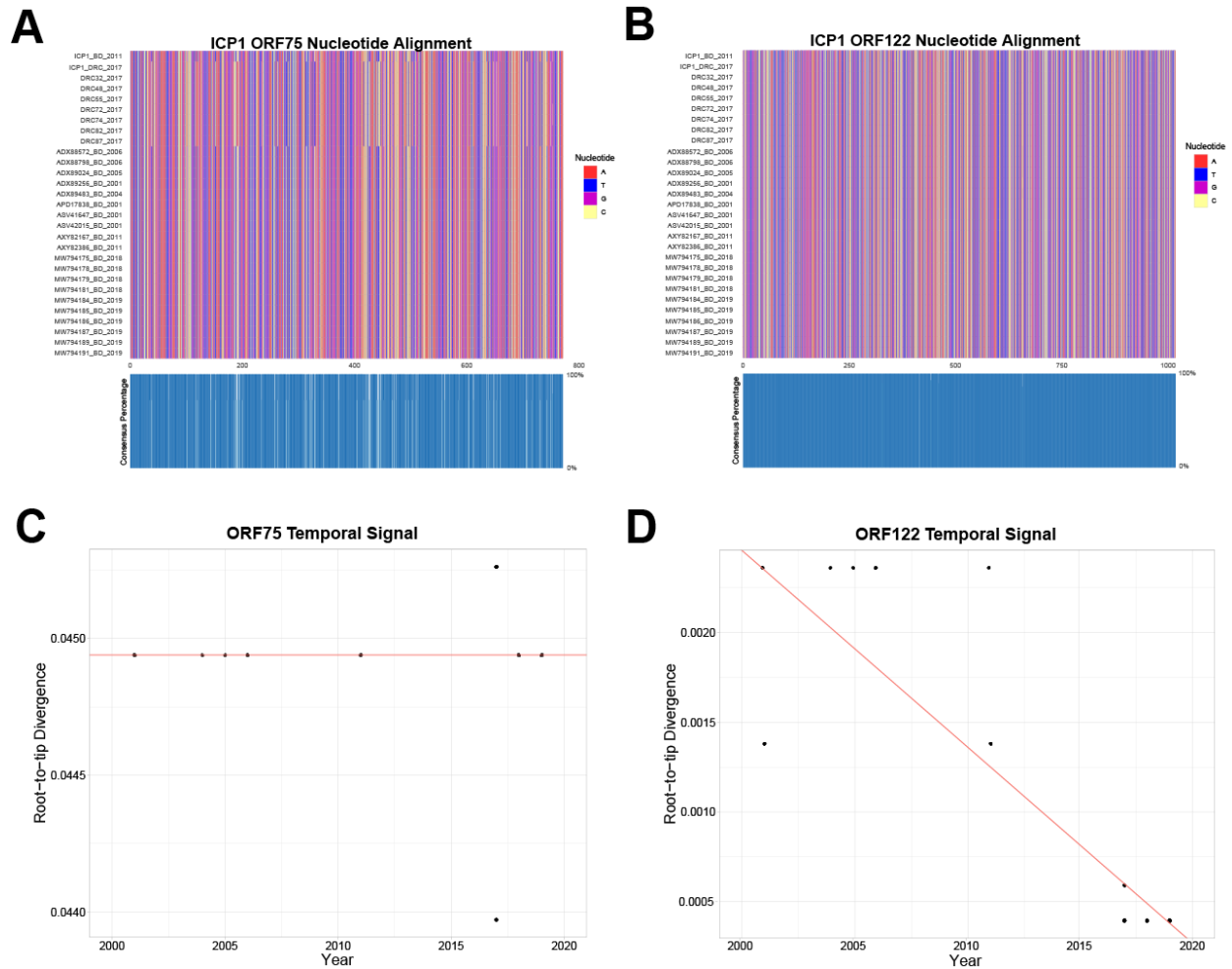
441 shown by symbols. The asterisk symbol represents identical amino acid, colon

442 represents similar amino acid and any gaps in the alignment represent mismatched

443 amino acid.



445 **Figure S2**



446

447 **Fig S2.** Multi-sequence alignment of ICP1 phage baseplate ORF75 **(A)** and capsular

448 head ORF122 **(B)** nucleotide sequences. Sequences from both Bangladesh (BD) and

449 Democratic Republic of Congo (DRC). Blue boxes at the bottom of A and B represent

450 the percentage of the isolates that have the same nucleotide for that particular site.

451 Temporal and divergence analysis of baseplate ORF75 **(C)** and capsular head ORF122

452 **(D)** nucleotide sequences from ICP1 strains isolated in Bangladesh.

453

454

455 **Table S1.** Microbiologic and molecular reagents

<b>Reagent</b>			
<b>Bacteria</b>	<b>Strain</b>	<b>Description</b>	<b>Reference</b>
<i>V. cholerae</i>	HC1037	O1 Ogawa serogroup, isolated from Haiti, SmR	(53)
<b>Bacteriophage</b>	<b>Strain (host)</b>	<b>Description</b>	<b>Reference</b>
ICP1	ICP1_2011_A ( <i>V. cholerae</i> O1)	<i>Myoviridae</i> , isolated from Bangladesh	(14)
ICP1	ICP1_DRC_106 ( <i>V. cholerae</i> O1)	<i>Myoviridae</i> , isolated from Goma, DRC	(19)
ICP2	ICP2_2004_A ( <i>V. cholerae</i> O1 and non-O1)	<i>Podoviridae</i> , isolated from Bangladesh	(14)
ICP3	ICP3_2007_A ( <i>V. cholerae</i> O1 and non-O1)	<i>Podoviridae</i> , isolated from Bangladesh	(14)

456  
457  
458  
459

460 **Table S2.** List of immunogenic ICP1 core ORFs.  
461

Predicted Protein	Function	Predicted Antigenicity (rank) <sup>a</sup>	Length (nt)	No of predicted epitopes <sup>b</sup>	Length (aa)
ORF66	hypothetical protein	1.03 (1)	228	3	75
ORF154	hypothetical protein	0.92 (2)	132	1	43
ORF158	hypothetical protein	0.83 (3)	258	3	85
ORF9	hypothetical protein	0.81 (4)	159	2	52
ORF206	hypothetical protein	0.77 (5)	219	3	72
ORF214	hypothetical protein	0.75 (6)	189	3	62
ORF75	putative baseplate assembly protein	0.73 (7)	774	7	257
ORF1	hypothetical protein	0.73 (8)	108	1	35
ORF195	hypothetical protein	0.71 (9)	162	2	53
ORF52	hypothetical protein	0.67 (10)	183	4	60
ORF122 <sup>c</sup>	putative major head protein	0.54 (17)	1020	14	339

462 <sup>a</sup> Predicted antigenicity score of initially selected 11 ORFs by Vaxijen v2. The threshold for this model is  
463 0.4 for a probable antigen. The rank is based on the antigenic score among 50 core ORFs (49 conserved  
464 core and 1 divergent core (c)) of ICP1 bacteriophage (17).

465 <sup>b</sup> Number of predicted B-cell epitopes by IEDB analysis. This analysis was done using Bepipred Linear  
466 Epitope Prediction 2.0 model.

467

468 **Table S3.** Molecular screening for predicted immunogenic targets in cholera and non-  
 469 cholera stools.

470

<b>Bangladesh samples</b>	ID	ORF75 <sup>a</sup>	ORF122 <sup>b</sup> ,
<i>V. cholerae</i> negative samples (n=10)			
S1	RN22	-	-
S2	RN23	-	-
S3	RN24	-	-
S4	RN25	-	-
S5	RN26	-	-
S6	RN27	-	-
S7	RN28	-	-
S8	RN29	-	-
S9	RN30	-	-
S10	RN31	-	-
<i>V. cholerae</i> positive samples (n=2)			
S1 (ICP1-)	RN3	-	-
S2 (ICP1+)	VCP 12	+	+
<b>South Sudan samples</b>			
Random <i>V. cholerae</i> negative sample (n=2)			
S1	1001	-	-
S2	1002	-	-
<i>V. cholerae</i> positive sample (n=2)			
S1 (ICP1-)	1008	-	-
S2 (ICP1+)	1086	+	+

471

472 <sup>a</sup> represents the PCR amplification results for the target ORF75, a putative baseplate protein

473 <sup>b</sup> represents the PCR amplification results for the target ORF122, a putative ICP1 bacteriophage head  
 474 protein.

475

## 476 REFERENCES

- 477 1. **Anonymous.** 2017. Cholera, 2016. *Wkly Epidemiol Rec* **92**:521-530.
- 478 2. **Azman AS, Moore SM, Lessler J.** 2020. Surveillance and the global fight against cholera: Setting  
479 priorities and tracking progress. *Vaccine* **38 Suppl 1**:A28-A30.
- 480 3. **Emch M, Feldacker C, Islam MS, Ali M.** 2008. Seasonality of cholera from 1974 to 2005: a review  
481 of global patterns. *Int J Health Geogr* **7**:31.
- 482 4. **Ganesan D, Gupta SS, Legros D.** 2020. Cholera surveillance and estimation of burden of cholera.  
483 *Vaccine* **38 Suppl 1**:A13-A17.
- 484 5. **Ali M, Nelson AR, Lopez AL, Sack DA.** 2015. Updated global burden of cholera in endemic  
485 countries. *PLoS Negl Trop Dis* **9**:e0003832.
- 486 6. **Cash RA, Narasimhan V.** 2000. Impediments to global surveillance of infectious diseases:  
487 consequences of open reporting in a global economy. *Bull World Health Organ* **78**:1358-1367.
- 488 7. **Zumla A, Hui DSC.** 2019. Emerging and Reemerging Infectious Diseases: Global Overview. *Infect*  
489 *Dis Clin North Am* **33**:xiii-xix.
- 490 8. **Clemens JD, Nair GB, Ahmed T, Qadri F, Holmgren J.** 2017. Cholera. *Lancet* **390**:1539-1549.
- 491 9. **Harris JB, LaRocque RC, Qadri F, Ryan ET, Calderwood SB.** 2012. Cholera. *Lancet* **379**:2466-  
492 2476.
- 493 10. **Nelson EJ, Chowdhury A, Flynn J, Schild S, Bourassa L, Shao Y, LaRocque RC, Calderwood SB,**  
494 **Qadri F, Camilli A.** 2008. Transmission of *Vibrio cholerae* is antagonized by lytic phage and entry  
495 into the aquatic environment. *PLoS Pathog* **4**:e1000187.
- 496 11. **Faruque SM, Islam MJ, Ahmad QS, Faruque AS, Sack DA, Nair GB, Mekalanos JJ.** 2005. Self-  
497 limiting nature of seasonal cholera epidemics: Role of host-mediated amplification of phage.  
498 *Proc Natl Acad Sci U S A* **102**:6119-6124.
- 499 12. **Faruque SM, Naser IB, Islam MJ, Faruque AS, Ghosh AN, Nair GB, Sack DA, Mekalanos JJ.** 2005.  
500 Seasonal epidemics of cholera inversely correlate with the prevalence of environmental cholera  
501 phages. *Proc Natl Acad Sci U S A* **102**:1702-1707.
- 502 13. **Faruque SM.** 2014. Role of phages in the epidemiology of cholera. *Curr Top Microbiol Immunol*  
503 **379**:165-180.
- 504 14. **Seed KD, Bodi KL, Kropinski AM, Ackermann HW, Calderwood SB, Qadri F, Camilli A.** 2011.  
505 Evidence of a dominant lineage of *Vibrio cholerae*-specific lytic bacteriophages shed by cholera  
506 patients over a 10-year period in Dhaka, Bangladesh. *mBio* **2**:e00334-00310.
- 507 15. **Yen M, Cairns LS, Camilli A.** 2017. A cocktail of three virulent bacteriophages prevents *Vibrio*  
508 *cholerae* infection in animal models. *Nat Commun* **8**:14187.
- 509 16. **Nelson EJ, Grembi JA, Chao DL, Andrews JR, Alexandrova L, Rodriguez PH, Ramachandran VV,**  
510 **Sayeed MA, Wamala JF, Debes AK, Sack DA, Hryckowian AJ, Haque F, Khatun S, Rahman M,**  
511 **Chien A, Spormann AM, Schoolnik GK.** 2020. Gold Standard Cholera Diagnostics Are Tarnished  
512 by Lytic Bacteriophage and Antibiotics. *J Clin Microbiol* **58**.
- 513 17. **Angermeyer A, Das MM, Singh DV, Seed KD.** 2018. Analysis of 19 Highly Conserved *Vibrio*  
514 *cholerae* Bacteriophages Isolated from Environmental and Patient Sources Over a Twelve-Year  
515 Period. *Viruses* **10**.
- 516 18. **Boyd CM, Angermeyer A, Hays SG, Barth ZK, Patel KM, Seed KD.** 2021. Bacteriophage ICP1: A  
517 Persistent Predator of *Vibrio cholerae*. *Annu Rev Virol* **8**:285-304.
- 518 19. **Alam MT, Mavian C, Salemi M, Tagliamonte MS, Paisie T, Cash MN, Angermeyer A, Seed KD,**  
519 **Camilli A, Maisha FM, Senga RKK, Morris JG, Ali A.** 2021. *Vibrio cholerae*  
520 multifaceted adaptive strategies in response to bacteriophage predation in an endemic region of  
521 the Democratic Republic of the Congo. *medRxiv*  
522 doi:10.1101/2021.07.30.21261389;2021.2007.2030.21261389.

- 523 20. **Anonymous.** Interim Guidance Document on Cholera Surveillance, Global Task Force on Cholera  
524 Control (GTFCC) Surveillance Working Group, WHO, June 2017  
525
- 526 21. **Tukei PM.** 1996. Emerging and re-emerging Infectious diseases: a global health threat. *Afr J*  
527 *Health Sci* **3**:27.
- 528 22. **Chibwe I, Kasambara W, Kagoli M, Milala H, Gondwe C, Azman AS.** 2020. Field Evaluation of  
529 Cholokit Rapid Diagnostic Test for *Vibrio Cholerae* O1 During a Cholera Outbreak in Malawi, 2018.  
530 *Open Forum Infect Dis* **7**:ofaa493.
- 531 23. **Page AL, Alberti KP, Mondonge V, Rauzier J, Quilici ML, Guerin PJ.** 2012. Evaluation of a rapid  
532 test for the diagnosis of cholera in the absence of a gold standard. *PLoS One* **7**:e37360.
- 533 24. **Dick MH, Guillerm M, Moussy F, Chagnat CL.** 2012. Review of two decades of cholera  
534 diagnostics--how far have we really come? *PLoS Negl Trop Dis* **6**:e1845.
- 535 25. **Sinha A, Sengupta S, Ghosh S, Basu S, Sur D, Kanungo S, Mukhopadhyay AK, Ramamurthy T,**  
536 **Nagamani K, Rao MN, Nandy RK.** 2012. Evaluation of a rapid dipstick test for identifying cholera  
537 cases during the outbreak. *Indian J Med Res* **135**:523-528.
- 538 26. **Debes AK, Ateudjieu J, Guenou E, Ebile W, Sonkoua IT, Njimbia AC, Steinwald P, Ram M, Sack**  
539 **DA.** 2016. Clinical and Environmental Surveillance for *Vibrio cholerae* in Resource Constrained  
540 Areas: Application During a 1-Year Surveillance in the Far North Region of Cameroon. *Am J Trop*  
541 *Med Hyg* **94**:537-543.
- 542 27. **Alam M, Hasan NA, Sultana M, Nair GB, Sadique A, Faruque AS, Endtz HP, Sack RB, Huq A,**  
543 **Colwell RR, Izumiya H, Morita M, Watanabe H, Cravioto A.** 2010. Diagnostic limitations to  
544 accurate diagnosis of cholera. *J Clin Microbiol* **48**:3918-3922.
- 545 28. **Sayeed MA, Islam K, Hossain M, Akter NJ, Alam MN, Sultana N, Khanam F, Kelly M, Charles RC,**  
546 **Kováč P, Xu P, Andrews JR, Calderwood SB, Amin J, Ryan ET, Qadri F.** 2018. Development of a  
547 new dipstick (Cholokit) for rapid detection of *Vibrio cholerae* O1 in acute watery diarrheal stools.  
548 *PLoS Negl Trop Dis* **12**:e0006286.
- 549 29. **Benenson AS, Islam MR, Greenough WB, 3rd.** 1964. Rapid Identification of *Vibrio Cholerae* by  
550 Darkfield Microscopy. *Bull World Health Organ* **30**:827-831.
- 551 30. **Bhuiyan NA, Qadri F, Faruque AS, Malek MA, Salam MA, Nato F, Fournier JM, Chanteau S, Sack**  
552 **DA, Balakrish Nair G.** 2003. Use of dipsticks for rapid diagnosis of cholera caused by *Vibrio*  
553 *cholerae* O1 and O139 from rectal swabs. *J Clin Microbiol* **41**:3939-3941.
- 554 31. **Nato F, Boutonnier A, Rajerison M, Grosjean P, Darteville S, Guérolé A, Bhuiyan NA, Sack DA,**  
555 **Nair GB, Fournier JM, Chanteau S.** 2003. One-step immunochromatographic dipstick tests for  
556 rapid detection of *Vibrio cholerae* O1 and O139 in stool samples. *Clin Diagn Lab Immunol*  
557 **10**:476-478.
- 558 32. **Qadri F, Hasan JA, Hossain J, Chowdhury A, Begum YA, Azim T, Loomis L, Sack RB, Albert MJ.**  
559 1995. Evaluation of the monoclonal antibody-based kit Bengal SMART for rapid detection of  
560 *Vibrio cholerae* O139 synonym Bengal in stool samples. *J Clin Microbiol* **33**:732-734.
- 561 33. **Haque F, Ball RL, Khatun S, Ahmed M, Kache S, Chisti MJ, Sarker SA, Maples SD, Pieri D,**  
562 **Vardhan Korrapati T, Sarnquist C, Federspiel N, Rahman MW, Andrews JR, Rahman M, Nelson**  
563 **EJ.** 2017. Evaluation of a Smartphone Decision-Support Tool for Diarrheal Disease Management  
564 in a Resource-Limited Setting. *PLoS Negl Trop Dis* **11**:e0005290.
- 565 34. **Ontweka LN, Deng LO, Rauzier J, Debes AK, Tadesse F, Parker LA, Wamala JF, Bior BK, Lasuba**  
566 **M, But AB, Grandesso F, Jamet C, Cohuet S, Ciglencecki I, Serafini M, Sack DA, Quilici ML,**  
567 **Azman AS, Luquero FJ, Page AL.** 2016. Cholera Rapid Test with Enrichment Step Has Diagnostic  
568 Performance Equivalent to Culture. *PLoS One* **11**:e0168257.
- 569 35. **Nelson EJ, Chowdhury A, Harris JB, Begum YA, Chowdhury F, Khan AI, Larocque RC, Bishop AL,**  
570 **Ryan ET, Camilli A, Qadri F, Calderwood SB.** 2007. Complexity of rice-water stool from patients



- 571 with *Vibrio cholerae* plays a role in the transmission of infectious diarrhea. Proc Natl Acad Sci U S  
572 A **104**:19091-19096.
- 573 36. **Hu YF, Zhao D, Yu XL, Hu YL, Li RC, Ge M, Xu TQ, Liu XB, Liao HY.** 2017. Identification of  
574 Bacterial Surface Antigens by Screening Peptide Phage Libraries Using Whole Bacteria Cell-  
575 Purified Antisera. Front Microbiol **8**:82.
- 576 37. **Mora M, Bensi G, Capo S, Falugi F, Zingaretti C, Manetti AG, Maggi T, Taddei AR, Grandi G,**  
577 **Telford JL.** 2005. Group A Streptococcus produce pilus-like structures containing protective  
578 antigens and Lancefield T antigens. Proc Natl Acad Sci U S A **102**:15641-15646.
- 579 38. **Gupta A, Grove A.** 2014. Ligand-binding pocket bridges DNA-binding and dimerization domains  
580 of the urate-responsive MarR homologue MftR from Burkholderia thailandensis. Biochemistry  
581 **53**:4368-4380.
- 582 39. **Sayed MA, Bufano MK, Xu P, Eckhoff G, Charles RC, Alam MM, Sultana T, Rashu MR, Berger**  
583 **A, Gonzalez-Escobedo G, Mandlik A, Bhuiyan TR, Leung DT, LaRocque RC, Harris JB,**  
584 **Calderwood SB, Qadri F, Vann WF, Kovac P, Ryan ET.** 2015. A Cholera Conjugate Vaccine  
585 Containing O-specific Polysaccharide (OSP) of *V. cholerae* O1 Inaba and Recombinant Fragment  
586 of Tetanus Toxin Heavy Chain (OSP:rTTHc) Induces Serum, Memory and Lamina Proprial  
587 Responses against OSP and Is Protective in Mice. PLoS Negl Trop Dis **9**:e0003881.
- 588 40. **Kauffman RC, Bhuiyan TR, Nakajima R, Mayo-Smith LM, Rashu R, Hoq MR, Chowdhury F, Khan**  
589 **AI, Rahman A, Bhaumik SK, Harris L, O'Neal JT, Trost JF, Alam NH, Jasinskas A, Dotsey E, Kelly**  
590 **M, Charles RC, Xu P, Kovac P, Calderwood SB, Ryan ET, Felgner PL, Qadri F, Wrammert J, Harris**  
591 **JB.** 2016. Single-Cell Analysis of the Plasmablast Response to *Vibrio cholerae* Demonstrates  
592 Expansion of Cross-Reactive Memory B Cells. mBio **7**.
- 593 41. **Priyamvada L, Quicke KM, Hudson WH, Onlamoon N, Sewatanon J, Edupuganti S,**  
594 **Pattanapanyasat K, Chokephaibulkit K, Mulligan MJ, Wilson PC, Ahmed R, Suthar MS,**  
595 **Wrammert J.** 2016. Human antibody responses after dengue virus infection are highly cross-  
596 reactive to Zika virus. Proc Natl Acad Sci U S A **113**:7852-7857.
- 597 42. **Priyamvada L, Cho A, Onlamoon N, Zheng NY, Huang M, Kovalenkov Y, Chokephaibulkit K,**  
598 **Angkasekwinai N, Pattanapanyasat K, Ahmed R, Wilson PC, Wrammert J.** 2016. B Cell  
599 Responses during Secondary Dengue Virus Infection Are Dominated by Highly Cross-Reactive,  
600 Memory-Derived Plasmablasts. J Virol **90**:5574-5585.
- 601 43. **Doytchinova IA, Flower DR.** 2007. Vaxijen: a server for prediction of protective antigens,  
602 tumour antigens and subunit vaccines. BMC Bioinformatics **8**:4.
- 603 44. **Larsen JE, Lund O, Nielsen M.** 2006. Improved method for predicting linear B-cell epitopes.  
604 Immunome Res **2**:2.
- 605 45. **Nguyen LT, Schmidt HA, von Haeseler A, Minh BQ.** 2015. IQ-TREE: a fast and effective stochastic  
606 algorithm for estimating maximum-likelihood phylogenies. Mol Biol Evol **32**:268-274.
- 607 46. **Rambaut A, Lam TT, Max Carvalho L, Pybus OG.** 2016. Exploring the temporal structure of  
608 heterochronous sequences using TempEst (formerly Path-O-Gen). Virus Evol **2**:vew007.
- 609 47. **Villanueva RAM, Chen ZJ.** 2019. ggplot2: Elegant Graphics for Data Analysis (2nd ed.).  
610 Measurement: Interdisciplinary Research and Perspectives **17**:160-167.
- 611 48. **Carroll IM, Ringel-Kulka T, Ferrier L, Wu MC, Siddle JP, Bueno L, Ringel Y.** 2013. Fecal protease  
612 activity is associated with compositional alterations in the intestinal microbiota. PLoS One  
613 **8**:e78017.
- 614 49. **Funabashi R, Miyakawa K, Yamaoka Y, Yoshimura S, Yamane S, Jeremiah SS, Shimizu K, Ozawa**  
615 **H, Kawakami C, Usuku S, Tanaka N, Yamazaki E, Kimura H, Hasegawa H, Ryo A.** 2021.  
616 Development of highly sensitive and rapid antigen detection assay for diagnosis of COVID-19  
617 utilizing optical waveguide immunosensor. J Mol Cell Biol **13**:763-766.

- 618 50. **Majewska J, Kazmierczak Z, Lahutta K, Lecion D, Szymczak A, Miernikiewicz P, Drapala J,**  
619 **Harhala M, Marek-Bukowiec K, Jedruchniewicz N, Owczarek B, Gorski A, Dabrowska K.** 2019.  
620 Induction of Phage-Specific Antibodies by Two Therapeutic Staphylococcal Bacteriophages  
621 Administered per os. *Front Immunol* **10**:2607.
- 622 51. **Dabrowska K, Miernikiewicz P, Piotrowicz A, Hodyra K, Owczarek B, Lecion D, Kazmierczak Z,**  
623 **Letarov A, Gorski A.** 2014. Immunogenicity studies of proteins forming the T4 phage head  
624 surface. *J Virol* **88**:12551-12557.
- 625 52. **Jerne NK, Avegno P.** 1956. The development of the phage-inactivating properties of serum  
626 during the course of specific immunization of an animal: reversible and irreversible inactivation.  
627 *J Immunol* **76**:200-208.
- 628 53. **Reyes-Robles T, Dillard RS, Cairns LS, Silva-Valenzuela CA, Housman M, Ali A, Wright ER,**  
629 **Camilli A.** 2018. *Vibrio cholerae* Outer Membrane Vesicles Inhibit Bacteriophage Infection. *J*  
630 *Bacteriol* **200**.
- 631